A Comparative Study of Prenucleation on Zr and MgO Substrates by *ab initio* MD Simulations

C. M. Fang and Z. Fan
BCAST, Brunel University London, Uxbridge, UB8 3PH, UK

1. Introduction

The traditional wisdom for grain refiners is by selecting the most potent solid particles (*i.e.* having the least misfit between the substrate and the metal) [1,2]. A good example is the Mg-Zr grain refiner for Mg and Mg-alloys. Zr is iso-structural to Mg with a small lattice misfit (~0.7 % at room temperature) [3]. The melting temperature of Zr is 1855°C (2128 K), notably higher than that of Mg (649°C). Interestingly, Zr is chemically repulsive to Mg with a heat of mixing +6 kJ/mol, and there forms no Zr-Mg intermetallic compound [3,4]. Zr particles have been considered to be good for heterogeneous nucleation of Mg through structural templating according to the epitaxial nucleation model [5]. Recently, it was also suggested that the most effective grain refinement can be achieved by the least potent particles (*i.e.* having largest misfit) if no other more potent particles of significance exist in the melt [6]. The role of MgO in heterogeneous nucleation of Mg can be a good demonstration of this theory [6].

Magnesia (MgO) forms readily in liquid Mg and Mg-alloys due to the high affinity between O and Mg. It has a NaCl-type structure and is a typical ionic crystal. The stable surface of the ionic crystals is MX{001} which contains equal numbers of M^{n+} and X^{n-}. Therefore, MX{001} contains no net charges (i.e., non-polar). The flat MgO{001} in liquid Mg provides a good case of the 'hard wall' effect [7]. While, a cleavage of MX{111} produces two smooth surfaces with the M- or X-termination, which contains net charges (polar). The polar surfaces are unstable under ambient condition, but can be stabilized by defects, e.g. M or X domains [8-10]. However, the situation can be different for the MX in a (liquid) metal environment. The free electrons of metals diminish the polar effect and stabilize the surfaces, such as the case of MgO{111} in Mg. MgO{111} has a 2D hexagonal lattice, the similar to that of the dense Mg{0001} plane. However, the misfit between MgO{111} and Mg{0001} is large (8.19 % at 650°C). The L-Mg/MgO{111} system provides us with a good opportunity to investigate the structural effect on atomic ordering of liquid Mg adjacent to a liquid/substrate interface [6].

There have been both experimental and theoretical efforts to obtain insight into the nucleation of Mg during solidification of Mg-alloy melts [11-16]. Experiments showed that a small amount of Zr addition could dramatically reduce the grain size of Mg alloys [11]. High-resolution electron microscopy (HRTEM) observations provided a simple orientation relation between the substrate and metal, {0001}[11-20]Mg//{0001}[11-20]Zr [11]. HRTEM was also employed to study the as-cast Mg alloys. Both octahedral (denoted as MgO{111}) and cubic MgO (denoted as MgO{001}) were observed in Mg melts [12-14]. The observations produced orientation relations (OR) between the MgO substrates and the □-Mg [12-14]. Meanwhile, the orientation relations between Mg and MgO{001} are rather complex [12-14]. First-principles approaches were used to investigate but mainly the wetting and adhesion for different crystal orientations between solid Mg and MgO [15-

17]. Xu *et al.* reported that the effects of interfacial energy and epitaxial strain on interfacial crystal orientations [16]. First-principles study on Mg{0001}/MgO{111} interfaces suggested that the Mg-terminated {111} surface is more stable than the corresponding O-terminated one [17]. To understand structural effect on both prenucleation and nucleation at atomic level, Men and Fan performed atomistic MD simulations on the atomic arrangements of a liquid metal adjacent a substrate of different misfits in a systematic way. The simulations showed that structural effect is strong on the atomic in-plane ordering but weak on the atomic layering for liquid metals adjacent to the substrates. A substrate of a smaller misfit provides better structural templating for heterogeneous nucleation [18-20], in agreement with the epitaxial nucleation model [5]. Recently we investigated the chemical effect of substrates on the atomic arrangements in the liquid adjacent to the surface of a potent substrate and found that a chemically affinitive substrate enhances prenucleation whereas a chemically repulsive substrate weakens it [21]. Therefore, the L-Mg/Zr{0001} with a large repulsive nature to the liquid is of special interest.

In this paper, we investigate the atomic arrangements of liquid Mg adjacent to three typical substrates through a comparative approach: i) liquid Mg on the potent, but chemically repulsive Zr{0001} substrate; ii) liquid Mg on the polar MgO{111} substrate; and iii) liquid Mg on a non-polar MgO{001} substrate using a parameter-free *ab initio* MD technique. Our simulations show a general trend of prenucleation phenomena of Mg liquid on the three typical substrates. The geometries of the substrate surfaces have been analysed. The obtained information is not only helpful to understand solidification of Mg, but also to get some insight into heterogeneous nucleation processes in general.

2. *Ab initio* approach

A hexagonal supercell with $a = 5a_h$ ($a_h = (\sqrt{2}/2)a_o$, and a_o (= 4.213 Å [22]) is the lattice parameter of MgO) was built for the L-Mg/MgO{111} systems. The substrate is composed of four O layers and three Mg layers (O-terminated) or five Mg layers (Mg-terminated). The length of the *c*-axis is set to be in accordance to the density of liquid Mg [23]. In this way the hexagonal supercell has a_{sc} = 14.895 Å and c_{sc} = 64.624 Å, which contains 525 atoms (425 Mg and 100 O) for the L-Mg/MgO{111} systems. A tetragonal supercell ($a = 4a_o$ = 16.852 Å and c = 35.052 Å) was built for the L-Mg/MgO{001} system. This supercell contains 320 Mg as liquid, and 96 MgO as the substrate. For the L-Mg/Zr{0001} system we built a hexagonal supercell with $a = 5a_o$ = 16.289 Å and c = 58.141 Å, where a_o (= 3.2578 Å) is slightly larger than the room temperature value (3.232 Å) [3], considering the temperature effect [23,24]. This cell contains 100 Zr and 450 Mg atoms.

We employed the first-principles code VASP (Vienna *Ab initio* Simulation Package) [25,26] which uses the *ab initio* density functional theory (DFT) within the projector-augmented wave (PAW) framework [27,28]. The exchange and correlation terms were described using the generalized gradient approximation (GGA-PBE) [29]. The cut-off energies for the wave functions and for the augmentation functions were 550.0 eV and 700.0 eV, respectively. The electronic wave functions were sampled on dense grids, e.g. a 24×24×24 k-mesh (365 ***k***-points) in the irreducible Brillouin zone (BZ) for the conventional cell of MgO, using the Monkhorst and Pack method [30]. For *ab initio* MD of the large cells, we employed a cut-of energy of 240 eV and Γ-point in the BZs.

The liquid Mg part of the samples was generated by equilibrating for about 10 ps at 3000 K. Then the liquid slowly annealed to the designed temperature in order to eliminate defects created at high temperature. The obtained liquid Mg was inserted onto the substrates. Then the obtained samples were heated at the designed temperature for about 10 ps. It is well-known that for systems containing liquids, a meaningful statistical analysis cannot be drawn from a single model, and conclusions based on limited configuration-sampling might be misleading [21, 31]. In the present

study we used several different inputs and employed the time-averaged method and took sampling with over several ps (2000 to 3000 steps). Tests for different inputs confirmed the availability of this approach. All substrate and liquid atoms were fully relaxed during the simulations.

3. Results

First we address the L-Mg/MgO{111} interfaces from different inputs, that is liquid Mg on an O-terminated and on an Mg-terminated MgO{111} substrate (Figure 1). During the MD simulations, we observed that on the O-terminated MgO{111} substrate the liquid Mg atoms adjacent to the substrate were moving quickly and approaching to terminating O (Figure 1b). Then an Mg layer was formed as the new terminating layer of the substrate. This movement is companied by the movement of other Mg atoms, gradually forming layers of Mg on the substrate. This process happens in a rather short time (0.1 to 0.3 ps). Careful analysis showed that there are holes at the newly formed Mg layer with a smaller number of Mg atoms as compared with that of the corresponding O atoms. For L-Mg/MgO{111}-system during the MD simulations some terminating Mg atoms/ions were gradually moving away and joining the liquid (Figure 1a). As a result, the terminating Mg layer contains holes, as well. Analysis showed that after certain period (1 ps) there is no notable difference for the simulated systems from the two inputs. The newly formed Mg layer terminates the MgO{111} substrate and behaves as templating for the adjacent liquid Mg atoms.

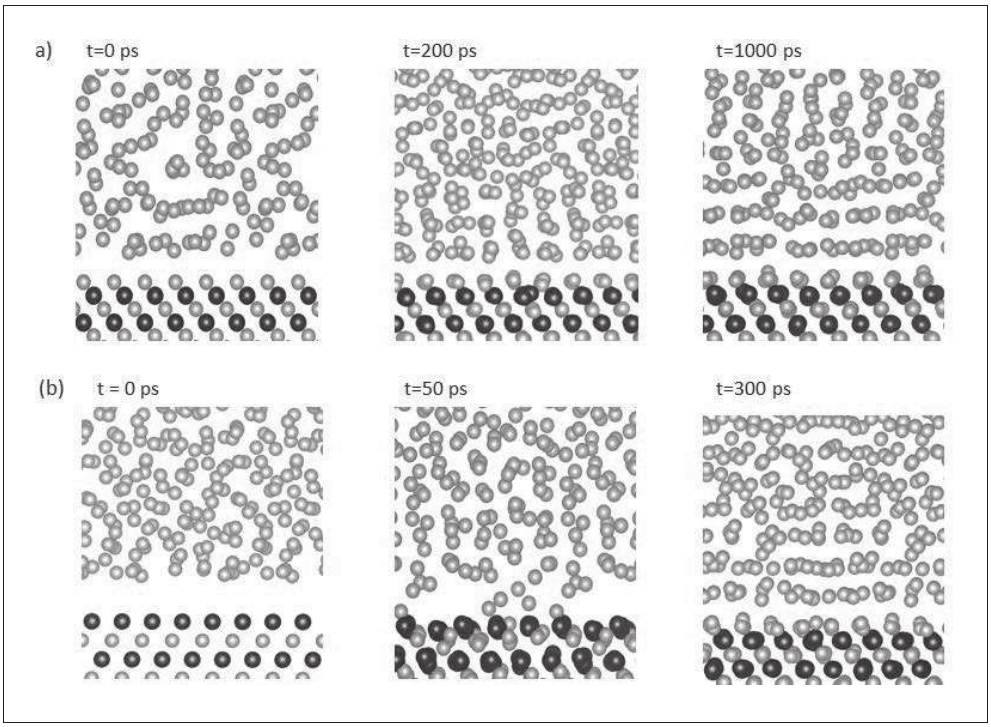

Figure 1: The formation of 2D structure at the MgO{111} substrate in liquid Mg with (a) the input being Mg-terminated substrate, L-Mg/MgO{111}$_{Mg}$ and (b) the input being O-terminated substrate, L-Mg/MgO{111}$_{O}$. The orange spheres represent Mg and dark blue for O.

Now we discuss the atomic arrangements of liquid Mg adjacent to the three types of substrates simulated at 1000K. Figure 2 shows snapshots for the liquid Mg on the MgO{001} (Fig. 2b) and the MgO{111} (Fig. 2c) substrates, as well as on the Zr{0001} (Fig. 2a) for the purpose of comparison.

From Figure 2 we can observe the following phenomena: i) on the potent substrate Zr{0001}, the Mg atoms exhibit clear layering (three distinct Mg layers, Figure 2a). This is similar to that of the L-Al/S-Cd system [21]. This is understandable because both L-Mg/Zr{0001} and L-Al/Cd{0001} systems have a chemical repulsive nature; the heat of mixing for the Mg/Zr system is +6 kJ/mol and that for the Al/Cd system is +3.0 kJ/mol [3]), the difference in chemical repulsion results in a larger interlayer Mg-Zr spacing than the Al-Cd spacing; and larger interlay spacing weakens atomic layering [21]. Meanwhile, the larger interlay spacing for Mg{000} layers ($d_{Mg\{0001\}}$=2.61 Å) as compared with that of Al{111} ($d_{Al\{111\}}$=2.34 Å) indicates larger separation of the liquid layers. This compensates the reduction of layering due to the stronger repulsive nature of the L-Mg/r{0001} interface system. Figure 2 also shows that in the first layers adjacent to substrate these Mg atoms have little tendency to change their atomic positions with their neighbours, suggesting a reduced atomic mobility; ii) For the L-Mg/MgO{111} system of a large misfit, the substrate is terminated by a Mg layer which contains defects. Some of the terminating Mg atoms are also out of the plane, causing certain degree of roughness (Figure 2c). There is but only one or two well identifiable layer(s) for liquid Mg near the substrate. These Mg atoms in the layer(s) show position changes with each other and are mainly of liquid nature; iii) There is a distinct separation between the liquid Mg atoms and the MgO{001}. However, the liquid Mg atoms adjacent to the substrate show no clear layering phenomenon (Figure 2b).

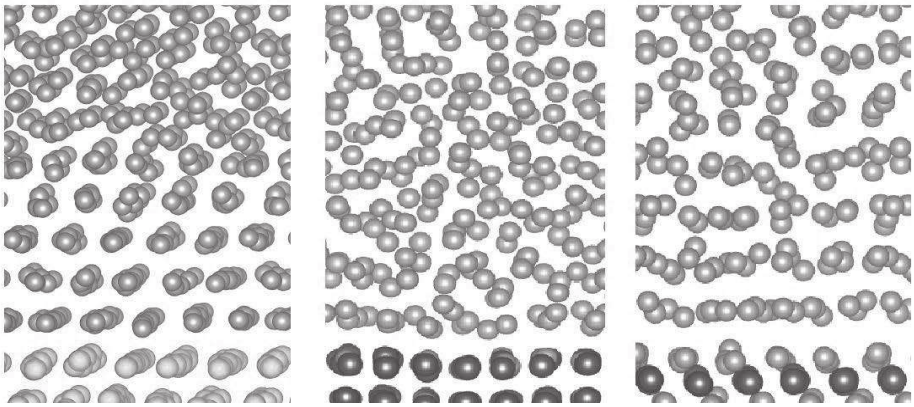

Figure 2: Snapshots for the liquid Mg atoms on: (a) Zr{0001}, (b) MgO{001} and (c) MgO{111} substrates simulated at 1000 K. The black spheres represent O, orange Mg and green for Zr.

The density profile of liquid perpendicular to a substrate surface, ρ(z) provides a quantitative description of the atomic layering phenomenon [18-21]. We analysed the density profiles for the time averaged atomic configurations of the simulated systems for over 3 ps. The density profiles ρ(z) and related peak heights were plotted in Figure 3.

Resultant density profiles confirmed our first impressions about the layering phenomenon in Figure 2. For the L-Mg/Zr{0001} system, though the peak-height of the outmost layer of Zr substrate

is rather low (0.44 $Å^{-3}$), there are 6 liquid Mg peaks (Figure 3a). The first three Mg layers are sharp and have peak heights close to that of the solid Zr. The peak heights of the liquid Mg layers decrease with increasing distance away from the in the interface. For the L-Mg/MgO{111} system, there are only 3 Mg layers can be recognized. The peak heights are notably lowered than those of the L-Mg/Zr{0001} system though the peaks of the substrates have high values. For the L-Mg/MgO{001} system, the MgO{001} substrate doesn't promote the atomic layering of the liquid Mg. There are only two recognizable Mg peaks with low peak heights (Figure 3a). The interlayer spacing between the first Mg peak and second Mg peak in the L-Mg/MgO{001} system is the same as that of the L-Mg/MgO{111} system. A close look at the first liquid Mg peak of the L-Mg/MgO{001} system reveals that this Mg peak is asymmetrical as compared with that of the L-Mg/MgO{111} system. The 1st Mg peak in Figure 3a (top) extends notably more to the liquid side.

The atomic ordering of the Mg atoms in the layers adjacent to the substrates (in-plane ordering) is a good indicator for structural templating [18-21]. Here we analyse the overall behaviour of the Mg atoms in the first layers adjacent to the substrates. Figures 4 and 5 show the time-averaged atomic configurations of the outmost layer of substrates and the liquid Mg atomic layers adjacent to the interface; and corresponding in-plane ordering parameter, S(z).

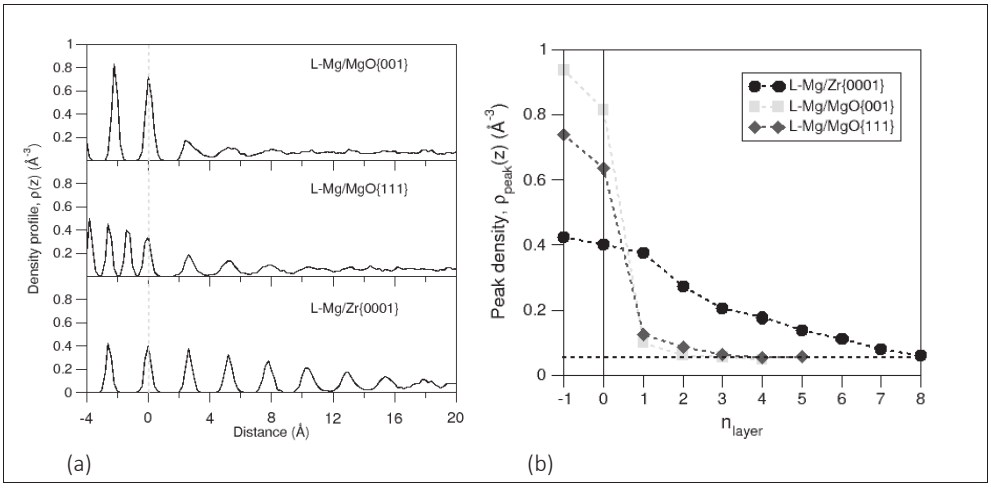

Figure 3: Atomic density profile, ρ(z) (left) and the peak heights of the liquid Mg (right) at 1000 K. The vetical dotted line (a) and filled line (b) are used to indicate the last peak of the substrates.

Figure 4 provides a direct picture about the atomic arrangement in the liquid adjacent to the substrates. The Mg atoms at the first three layers adjacent to the Zr{0001} substrate show localized atomic movements, in other words, they are more solid like. The Mg atoms in the fourth layer and beyond have higher atomic mobility suggesting they are more liquid like (Figure 4a). For the L-Mg/MgO{111} system, the outmost O atoms exhibit a well ordered solid structure. The first Mg layer also show solid-like behaviour and should be treated as the new terminating surface of the MgO{111} substrate. Interestingly this new terminating Mg layer contains significant amount vacancies at some lattice sites in addition to the fact that the terminating Mg atoms/ions also show roughness as some Mg atoms being off the plane (Figure 2c). As a consequence, the Mg atoms in the second layer are almost liquid like (Figure 4b). The Mg atoms in the first layer adjacent to the flat MgO{001} substrate exhibit no ordering and are also liquid-like (Figure 4c).

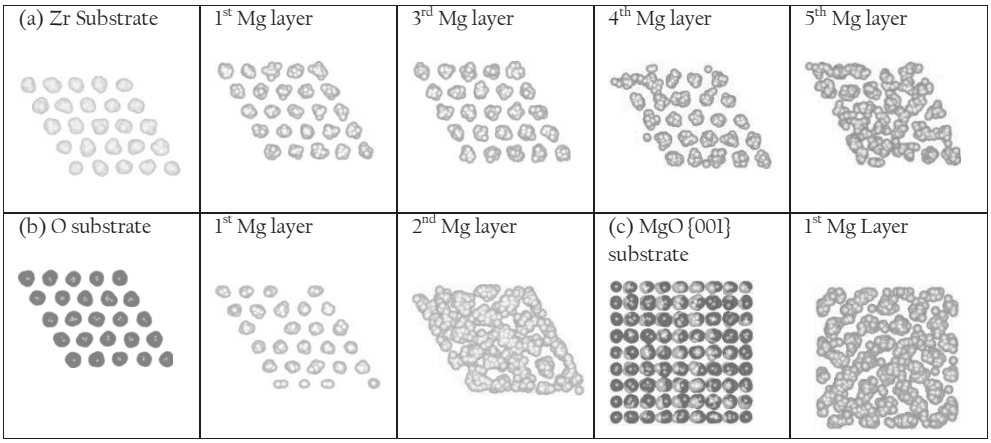

Figure 4: The time-averaged atomic configurations of the outmost layer of the substrate and the first few liquid Mg layers on the substrates at 1000 K: a) for L-Mg/Zr{0001}; and b) L-Mg/MgO{111} and c) L-Mg/MgO{001} systems.

The in-plane ordering coefficients for the integrated configurations of the L-Mg/Zr{0001} and L-Mg/Mg{111} systems are shown in Figure 5. The analysis showed that in-plane ordering coefficients of the atoms in the MgO{111} substrate are notably higher than those in the Zr substrates. This is consistent with their melting points (T_m = 1855 °C for Zr vs. T_m = 2852 °C for MgO). However, S(z) values of the Mg in the liquid adjacent to the substrate behave in a different way: S(z) = 0.42 for the first Mg layer on the Zr{0001} substrate. It decreases with the distance away from the interface, and approaching zero at the fifth layer, whereas S(z) is almost zero for the first Mg layer on MgO{111} substrate. Analysis also showed that S(z)≈0 for the first Mg layer on the flat MgO{001} substrate. Analysis also showed the peak density of Mg atoms in the first liquid Mg layer is about 0.105 $Å^{-2}$, which is close to that on the L-Mg on MgO{111} substrate.

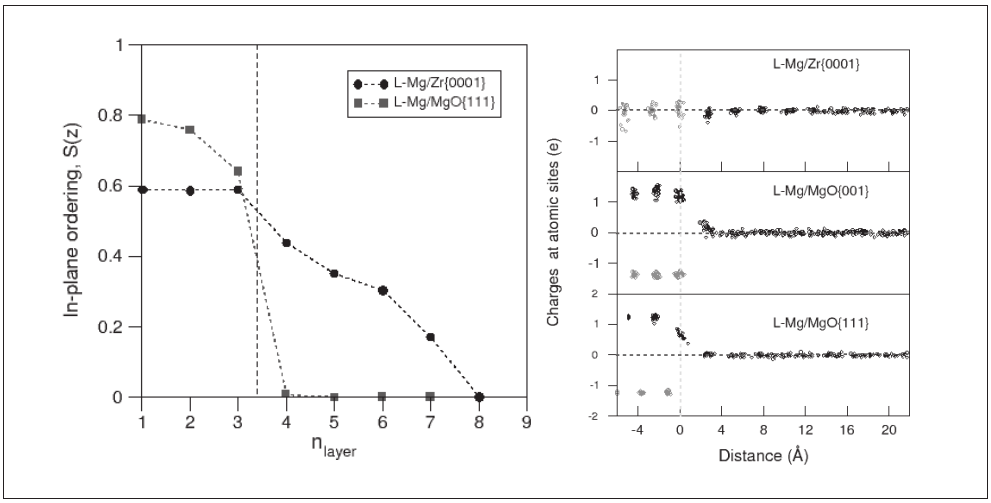

Figure 5: Left: In-plane order coefficients, S(z) for liquid Mg on the Zr{0001} substrate and on the MgO{111} substrate. The dotted vertical blue line indicates the border between substrate and liquid Mg. Right: The calculated charges at the atomic sites in the L-Mg/Zr{0001}, L-Mg/MgO{001} and L-Mg/MgO{111} systems.

Charge transfer is helpful to understand the interfacial interaction [21]. Figure 5b shows the charges at the atomic sites for the discussed systems using the Bader model [32] implanted in the code [33]. There is a little charge transfer (0.02e/Mg) from interfacial Mg to Zr, in consistence with their electronegativity (1.31 for Mg and 1.33 for Zr in Pauling scale). All O in MgO substrates have the same charge (-1.3e) and Mg in the substrates are positively charges with a loss of 1.3e/Mg. This agrees with the large electronegativity difference between Mg(1.31) and O (3.44). Figure 5b also shows that the terminating Mg ions to MgO{111} substrate are less charged (about +0.6e/Mg on average) as compared with those in the substrate. The Mg atoms at the first liquid layer (i.e., the 2nd Mg layer in Fig. 4b) on the MgO{111} substrate are electronically neutral. Interestingly, the Mg ions at the outmost of the MgO{001} substrate are less charged as compared to those in the substrate. The liquid Mg atoms adjacent to the substrate lose some electrons. This means that charge transfer occurs from the liquid Mg to the substrate.

Here we try to analyze the geometry of the MgO{001} surface in liquid Mg in detail. To provide more direct details about charges at the Mg metallic in liquid, Mg^{2+} and O^{2-} ions in the substrates, the iso-surfaces of electron density distribution of the L-Mg/MgO{001} is shown in Figure 6a.

Figure 6a confirms the ionic model of the substrate: the electron densities around the O^{2+} ions (the dark blue spheres) are very high. There are no notable electron clouds around the Mg ions in the substrate, whereas the electron clouds are clearly seen in the liquid Mg part. The latter corresponds to the free-electron behaviour of the alkaline metals. These results are consistent with the Bader charge analysis (Figure 5b). These results indicate that the MgO{001} surface is dominated by the large O^{2-} ions.

Figure 6b shows a snapshot of the atomic arrangements at the surface layer of MgO{001} substrate in liquid Mg. The ions are well ordered in this plane, in agreement with the integrated configurations in Figure 4c. Meanwhile, a close look at snapshot of the atomic arrangements including their heights perpendicular to the substrate reveals that the Mg and O ions in the surface plane have a broad variety of heights to the liquid Al (Figure 6c). Analysis showed that the differences in height of the ions can be as large as 0.5 Å. Figure 6d displays the statistics of the atomic heights of two close Mg (top) and two O (bottom) ions in the surface plane of the MgO{001} substrate on time. This figure provides that at a given moment, each ion in the surface plane displaces from its ideal position, or different heights of the surface ions at the MgO{001} surface. Therefore, the MgO{001} surface atomically rough when it is in contact with liquid Mg melts at high temperature. This can be understood that the surface ions have one less neighbours in the direction to the liquid as compared to those of bulk ones. This enhances displacements of the surface ions from their ideal positions at high temperature [4]. Furthermore, there is interaction between the O^{2-}, Mg^{2+} ions at the substrate with the liquid free-electron Mg atoms in liquid. Such interaction will cause the ions at the substrate surface displace more into the liquid. This atomic roughness of the MgO{001} substrate surface will further deteriorate the atomic layering and in-plane ordering of the liquid adjacent to the interface at the prenucleation stage, beyond the effect of large lattice mismatch.

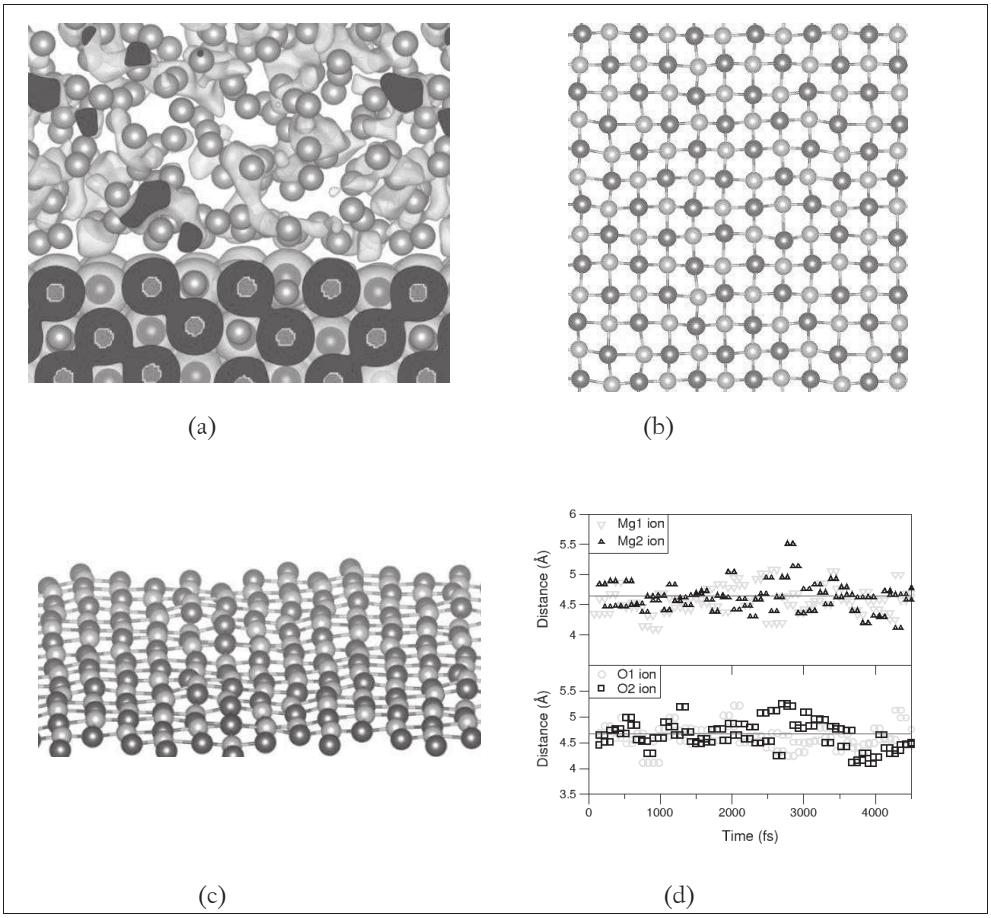

Figure 6: a) the iso-surfaces of electron density distribution; (b) atomic arrangements of the surface layer of the MgO{001} substrate; c) a close view of the atomic positions of the surface, a snapshot of the MgO{001} surface layer of the L-Mg/MgO{001} system; and d) variations of the ionic positions along the z-axis for two nearby surface O^{2+} and two Mg^{2+} ions on the substrate with time for the L-Mg/MgO{001}. In Figure 5a, the yellow spheres represent the iso-surfaces ($\rho(r)$=0.017 e/Å^3), the blue regions indicates higher electron density and the white for lower, whereas the red regions for the core of O ions.

4. Summary

In the present study we addressed the effect of substrate on prenucleation in the liquid adjacent to the liquid/substrate interface, including nucleation potency, chemical nature of the substrate, and interfacial bonding.

a) Zr{0001} is a good example of potent substrates and provides a good structural templating for prenucleation, in spite of its strong repulsive nature. The liquid atoms adjacent to the liquid/substrate interface exhibit clear layering and in-plane ordering. Such pronounced atomic ordering indicates smaller driving force for heterogeneous nucleation according to the epitaxial nucleation model [5]. This agrees with the experimental observations that Zr is an effective grain refiner [12-14]. This results also confirms that the chemical effect on prenucleation is secondary to the structural/geometric factor [21].

b) The misfit between Mg{0001} and MgO{111} is large (8.19 %). The simulations showed formation of an Mg layer which terminates the substrate. This Mg layer contains both 2 dimensional defects and roughness. As a consequence, the liquid Mg atoms adjacent to the L-Mg/MgO{111} interface only have a moderate layering and little in-plane ordering, suggesting that MgO{111} is not effective for structural templating. Nucleation on the MgO{111} substrate requires large driving forces (large undercooling).

c) MgO{001} surface is non-polar, which indicates weak interaction between metal and the substrate. The liquid Mg atoms adjacent to the substrate tend to form some layer but no in-plane atomic ordering. Our analysis showed that MgO{001} surface is atomically rough. The combination of a large lattice mismatch and atomic roughness weakens structural templating for prenucleation by the MgO{001} substrates.

The overall order series (from good to bad) for the prenucleation phenomenon is: L-Mg/Zr{0001}»L-Mg/MgO{111}›(L-Mg/MgO{001}. However, if the liquid contains no other more potent substrates, MgO particles dispersed by intensive melt shearing can be utilised for more effective grain refinement [6]. When the driving force is large enough, heterogeneous nucleation and grain initiation occur simultaneously and triggers an immediate recalescence. In this way MgO, can be an very effective grain refiner [6,13,14].

Acknowledgements

EPSRC is gratefully acknowledged for supporting the EPSRC Centre under grant EP/H026177/1.

References

1. K.F. Kelton, A.L. Greer, Nucleation in condensed Matter: Applications in materials and biology, Elsevier, Amsterdam, 2010.
2. Z. Fan, *et al*. Acta Mater. 84 (2015) 292-304.
3. W.B. Pearson, Handbook of lattice spacings and structures of metals and alloys, Pergamon Press, Oxford, 1967.
4. A. Takeuchi, A. Inoue, Mater. Trans. 46 (2005) 2817-2829.
5. Z. Fan, Metall. Mater. Trans. A 44 (2013) 1409-1418.
6. B. Jiang and Z. Fan, Proc.6th decennial intern. Conf. on solidification processing, 25-28 (2017) 61-65.
7. A. Hashibon, J. Adler, M.W. Finnis, W.D. Kaplan, Comp. Mater. Sci. 24 (2002) 443-452.
8. P. W. Tasker, Philos. Mag. A 39 (2919) 119-36.
9. C. M. Fang, *et al*. J. Am. Ceram. Soc. 83 (2000) 2082-84.
10. C. M. Fang, *et al*. ACS Nano 4 (2010) 211-218.
11. W. C. Yang, *et al*. Mater. Lett. 160 (2015) 263-267.
12. B. J. Kooi, *et al*. Appl. Phys. Lett. 89 (2006) 161914.
13. Z. Fan, *et al*. Acta Mater. 57 (2009) 4891-490.
14. Y. Wang, *et al*. Philos. Mag. Lett. 91 (2011) 516-529.
15. E. T. Dong, *et al*. J. Mater. Sci. 48 (2013) 6008-17.
16. W. W. Xu, *et al*. J. Alloys and Compounds 688 (2016) 1233-1240.
17. H.-Q. Song, *et al*. Modern Phys. Lett. 30 (2016) 165052.
18. H. Men, and Z. Fan, IOP Conf. Series-Mater. Sci Eng. 27 (2011) 012007.
19. H. Men, and Z. Fan, Comput. Mater. Sci., 85 (2014) 1-7.
20. H. Men,and Z. Fan, Proc. 6th decennial intern. Conf. solidification processing, 25-28 July, 2017; page 43-47.
21. C. M. Fang, H. Men,and Z. Fan, Proc. 6th decennial intern. Conf. solidification processing, 25-28 July, 2017; page 52-55.
22. R. G. Merryman and C. P. Kempter, J. Am. Ceram. Sco. 48 (1965) 202-205.
23. P.-F. Paradis and W.-K. Rhim, J. Mater. Research 14 (1999) 3713-3719.

24. P. J. McGonigal, A. D. Kirshenbaum and A. V. Grosse, J. Phys. Chem. 66 (1962) 737-741.
25. G. Kresse,J. Hafner, Phys. Rev. B 49 (1994) 14251-69.
26. G, Kresse, J. Furthmüller, Comput. Mater. Sci. (1996) 15-50.
27. P.E. Blöchl, Phys. Rev. B 50 (1994) 17953-79.
28. G. Kresse, J. Joubert, Phys. Rev. B 59 (1999) 1758-75.
29. J. P. Perdew, K. Burke, M. Ernzerhof, Phys. Rev. Lett. 77 (996) 3865-68.
30. H. J. Monkhorst, and J. D. Pack, Phys. Rev. B, 13 (1976) 5188-92.
31. L. E. Hintzsche, *et al*. Phys. Rev. B 88 (2013) 155204.
32. R. F. W. Bader, J. Phys. Chem. A 102 (1998) 7314-7323.
33. W. Tang, E. Sanville, and G. Henkelman, J. Phys.: Condens. Matter 21 (2009) 084204.
34. N. L. Alland, W. C. Mackrodt, J. Phys.: Condens. Matter 1 (1989) SB189.